

Effect of MDOF structures' optimal dampers on seismic fragility of piping

Woo Young Jung^{1a} and Bu Seog Ju^{*2}

¹Department of Civil Engineering, GangNeung-WonJu National University, GangNeung, Korea

²Department of Civil Engineering, North Carolina State University, Raleigh, USA

(Received July 18, 2014, Revised November 24, 2014, Accepted April 15, 2015)

Abstract. Over the past few decades, seismic retrofitting of structural systems has been significantly improved by the adoption of various methods such as FRP composite wraps, base isolation systems, and passive/active damper control systems. In parallel with this trend, probabilistic risk assessment (PRA) for structural and nonstructural components has become necessary for risk mitigation and the achievement of reliable designs in performance-based earthquake engineering. The primary objective of the present study was to evaluate the effect on piping fragility at T-joints due to seismic retrofitting of structural systems with passive energy-dissipation devices (i.e., linear viscous dampers). Three mid-rise building types were considered: without any seismic retrofitting; with distributed damper systems; with optimal placement of dampers. The results showed that the probability of piping system failure was considerably reduced in a Multi Degree of Freedom (MDOF) building retrofitted with optimal passive damper systems at lower floor levels. This effect of damper systems on piping fragility became insignificant as the floor level increased.

Keywords: passive dampers; piping; fragility; SSSA; earthquake

1. Introduction

Critical facilities such as nuclear power plants, hospital buildings, high-tech factories and emergency management building systems have rigorous seismic performance requirements both during and after an earthquake. Some structures in current critical facilities were designed based on old (i.e., less rigorous) seismic safety criteria; as such, in order to satisfy the present requirements, they need to be retrofitted or strengthened by fiber wrapping, steel jacketing, and a passive damper control system, (Parulekar *et al.* 2009). Traditional seismic guidelines have devoted more thorough and detailed attention to structural systems than to nonstructural components such as mechanical and electrical equipment, medical equipment, and plumbing and piping systems. Even so, poorly performing nonstructural components have been the most common causes of earthquakes and their destructive effects, which include direct property damage, operational/functional interruption, and loss of life (Gould and Griffin, 2003). In fact,

*Corresponding author, Ph.D., E-mail: bjju2@ncsu.edu

^aProfessor, E-mail: woojung@gwnu.ac.kr

nonstructural components are much more vulnerable than structural systems during an earthquake.

The Northridge earthquake of 1994, for example, caused no structural damage to the Olive View Medical Center in Sylmar, CA, USA. Instead, water leakage from broken fire-protection sprinkler piping and damaged chilled-water systems wrought greater damage by shutting down operations and, in turn, forcing patients to be evacuated (Reitheman and Sabol 1995). Furthermore, of the approximate \$6.3 billion of direct economic loss to nonresidential buildings incurred as a result of that earthquake, only about \$1.1 billion was due to structural damage (Kircher 2003). Indeed, the Northridge earthquake is instructive as an illustration of the significantly higher economic loss typically due to nonstructural damage.

In recent years, many engineers have recognized a need to address these problems at the design stages, their objective being to enable nonstructural components to remain operational and/or functional after an earthquake. In order to achieve reliable design of a piping system as a nonstructural component for example, Ju and Jung (2013) evaluated the seismic fragility of the system as installed at each floor level in low-rise buildings. Later, Ju *et al.* (2013) reported the results of an analysis of top-floor piping fragilities as a function of building height and building type.

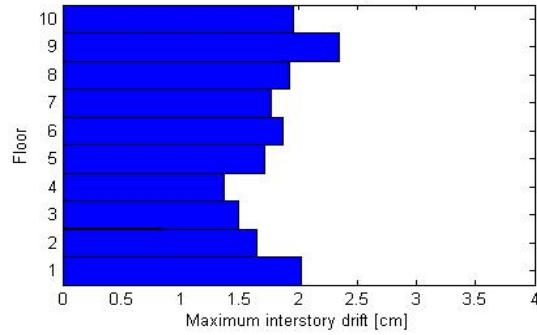
The current study was a continuation of those two previous investigations (Ju and Jung 2013, Ju *et al.* 2013). Its primary objective was to investigate the effect on nonstructural components (piping systems) due to optimal damper allocations in a Multi Degree of Freedom (MDOF) building. The particular focus was the evaluation of the system-level fragilities of the piping system installed in three different building types: a regular mid-rise building without any seismic retrofit, a building with distributed linear viscous dampers, and a building with optimal damper allocations. The evaluation proceeded on the basis of nonlinear acceleration time-histories using a Monte-Carlo simulation that accounted for ground-motion uncertainties.

2. Overview of linear frame building

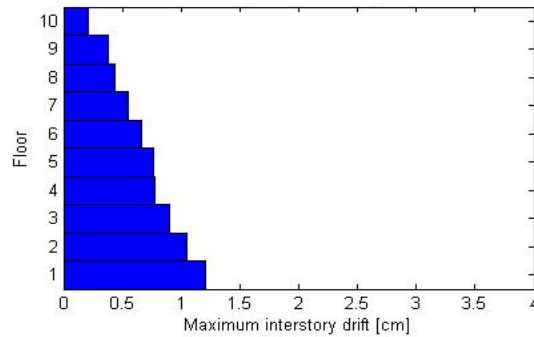
2.1 MDOF building system and optimal damper allocations

For the purposes of the present seismic retrofitting, the 10-story building model proposed by Garcia and Soong (2002) was used to simulate different earthquake ground motions. According to Garcia and Soong (2002), for the design of optimal damper allocation, their proposed Simplified Sequential Search Algorithm (SSSA) was employed. Specifically, the SSSA was applied to several regular building models with different natural periods, numbers of stories, levels of added damping, and different ground motions for a passive energy-dissipation device considering only linear viscous damping. In the present study, lumped mass and equivalent loads were used for 10-story linear frame building models. The damping ratio using mass and stiffness proportional Rayleigh damping in all modes distributing to the response in steel frame models was taken as 2%. Three different values of stiffness property for the building system were applied: 1000 (KN/cm) up to the 4th floor; 850 (KN/cm) up to the 8th floor; 720 (KN/cm) up to the 10th floor. Additionally, following Garcia and Soong (2002)'s recommendation, the damping coefficient (c) was estimated using the approximate equation

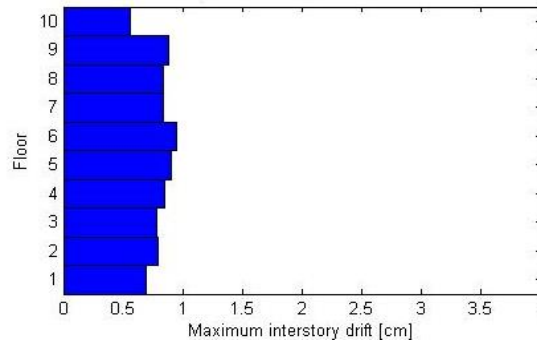
$$c = \frac{\xi_d T \sum_{i=1}^n k_i}{\pi \cdot n_d} \quad (1)$$



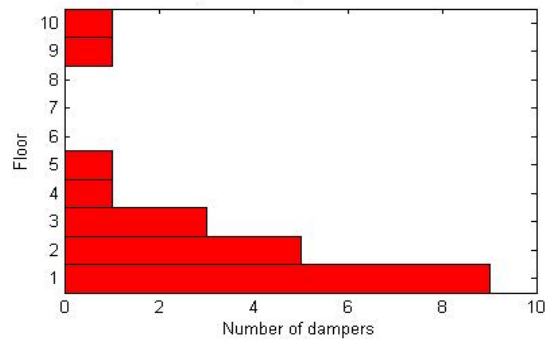
(a) Interstory drift: Structure without dampers



(b) Interstory drift: Structure with distributed dampers



(c) Interstory drift: Structure with optimized dampers



(d) Location of optimized dampers in building

Fig. 1 Building drift ratio and optimized damper allocations (Garcia and Soong 2002)

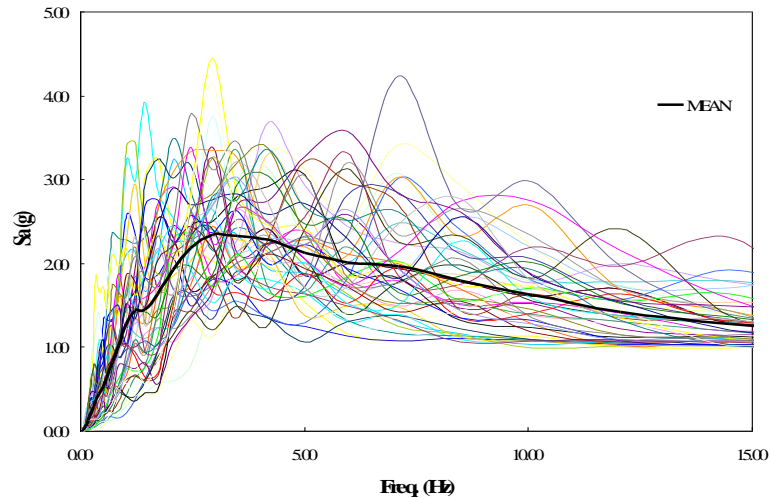


Fig. 2 Response spectra of selected ground motions (Ju and Jung 2013)

where,

ξ_d :	equivalent damping ratio due to the action of the added dampers
T:	fundamental natural period
k_i :	lateral stiffness of the i^{th} story
n_d :	number of dampers

Eq. (1) was applied under the assumption that 21 linear viscous dampers were used and that the maximum interstory drift ratio, based on UBC (1997), was 2% ($\Delta_{\max} = 1.5 \text{ cm}$). Further details on the damper systems can be found in Garcia and Soong (2002).

Fig. 1 shows the interstory drift responses and optimal damper allocations in the MDOF building subjected to the ground motions. As can be seen in Fig. 1, the interstory drift was significantly reduced for the structures having dampers optimally distributed according to the SSSA, which allocation is indicated in Fig. 1(d).

2.2 Seismic ground motions

In an evaluation of the optimal linear viscous damper allocation and system-level piping fragilities, 50 earthquakes as a function of ground-motion uncertainty were applied, as proposed by Ju and Jung (2013). The earthquake data were normalized to the same Peak Ground Acceleration (PGA) level. The response spectra for the 50 seismic events according to the 5% damping ratio are plotted in Fig. 2.

3. Nonstructural component: Piping system

The efficiency of the seismic retrofit of the damper systems in the MDOF building subjected to earthquake ground motions was evaluated with respect to Ju and Jung (2013)'s main piping system

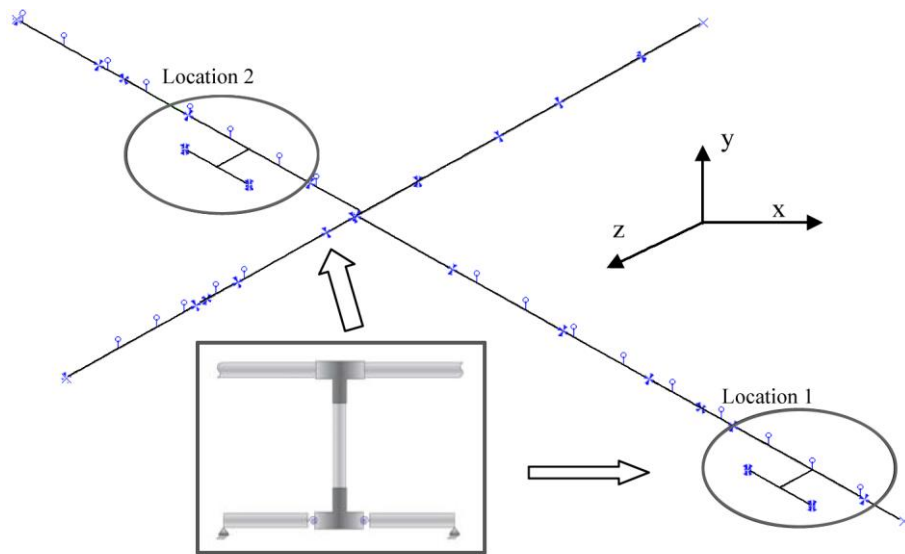


Fig. 3 Real piping system layout (Ju and Jung 2013)

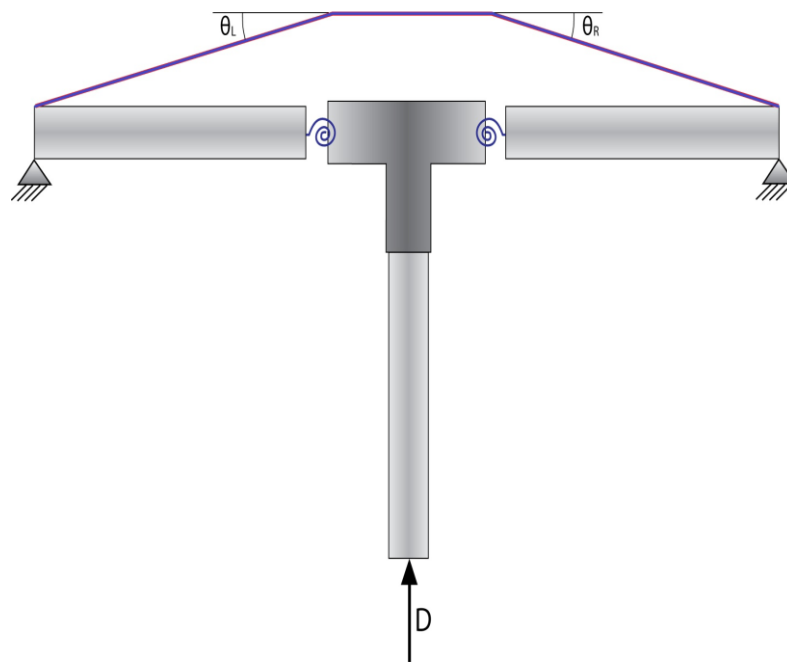


Fig. 4 FE model of T-joint piping system (Ju *et al.* 2011)

with two nonlinear T-joint branch systems as a nonstructural component.

3.1 Piping system layout

This main piping system, consisting of 2-4-inch black-iron pipes, was supported by unbraced single hangers, transverse-braced hangers and longitudinal-braced hangers modified to satisfy the seismic design guidelines of NFPA-13 (2007) and SMACNA (2003); at the ends of the system were 4 anchors. The particular locations of multi-branch piping systems consisting of 2-inch schedule 40 black-iron pipes were considered to determine the system-fragility levels, as based on the results of a linear time-history analysis of the complete piping system. In other words, the specific critical locations were determined as the first and second maximum displacements and rotations from linear time-history analyses on the main piping system without the multi-branch sub-systems. Fig. 3 shows the piping system resulted in the large energy absorption configuration with the natural frequencies of the fundamental and second modes, 1.82 (Hz) and 3.28 (Hz), respectively.

3.2 Finite Element (FE) model of nonlinear T-joint piping system

A nonlinear moment-rotation relationship derived from cyclic-experimental data obtained by the University of Buffalo (UB) (Dow 2010) was used to create the nonlinear Finite Element (FE) model of the threaded T-joint 2-inch black-iron branch piping system. The typical failure modes of the system were characterized as bending of pipe ends and slippage and rupture of pipe threads. Fig. 4's schematic representation of the FE model describes the nonlinear behavior as modeled by the two nonlinear rotational springs and specified by the moment-rotation relationships. The branch pipes were supported by a hinge at the end to allow for small rotations. The load was applied axially at the bottom along the perpendicular axis. In this particular T-joint FE model, the *Pinching4* uniaxial model was applied in the *OpenSees* (2011) platform. The *Pinching4* material model was able to represent the stiffness degradation, the strength degradation, and the unloading/reloading condition under cyclic loading. The FE model of the threaded T-joint is validated in Fig. 5. As is indicated, the FE model values were in good agreement with the experimental values. Further details on this FE model can be found in Ju *et al.* (2011).

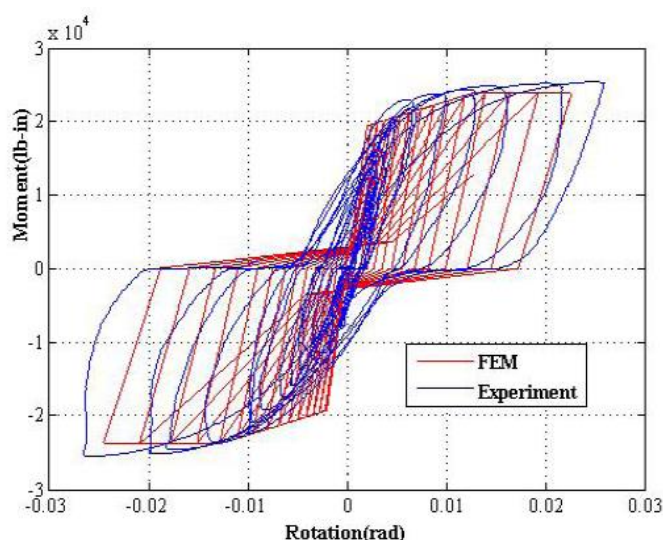


Fig. 5 Validation of FE model of 2-inch threaded T-joint system (Ju *et al.* 2011)

4. Probabilistic Risk Assessment (PRA): Piping fragility

4.1 Definition of seismic fragility

Over the last few years, the concept of seismic fragility has been applied to various structural and nonstructural systems such as nuclear power plants, bridges, buildings, and piping systems (Balasubramanian *et al.* 2014, Gardoni and Trejo 2013, Karantoni *et al.* 2014, Kibboua *et al.* 2011, Mehani *et al.* 2013, Park and Choi 2011, Perotti *et al.* 2013). Kennedy *et al.* (1980) developed uncertainty principles for ground-motion probability estimation and the conditional probability of structural failure estimation using a lognormal distribution in a nuclear power plant. Also, Porter and Bachman (2006) analyzed the damage state and fragility function of nonstructural components as compound lognormal distributions. Ju *et al.* (2011) defined the seismic fragility and damage state of the piping system as follows: nonstructural fragilities are functions that relate to probability, in that a nonstructural component exceeds a certain level of damage (DM) as a function of the Engineering Demand Parameter (EDP) (Bachman *et al.* 2004). Eq. (2) expresses fragility at a PGA level of λ as

$$P_f(\lambda) = P[EDPs \geq DM \mid PGA = \lambda] \quad (2)$$

Structural fragility in the present study was estimated empirically, through multiple nonlinear time-history analyses of the structure for various ground motions, as

$$P_f(\lambda) = \frac{\sum_{i=1}^N 1(\theta_{i,\lambda} \geq \theta_{\text{lim}} \mid PGA = \lambda)}{N} \quad (3)$$

where $\theta_{i,\lambda}$ is the maximum rotation from the i^{th} earthquake time-history analysis at a PGA level of λ , and $1(\cdot)$ is the indicator function (Ju *et al.* 2011).

4.2 Definition of limit state of piping system

According to the definition of fragility (Ju *et al.* 2011), it is necessary to characterize the limit-state criteria corresponding to the given damage. Generally, failure due to leakage precedes support-system failure. Therefore, Section III of the ASME BPVP code (2004) defines the rotation corresponding to plastic collapse of piping components according to the "Twice the Elastic Slope" (TES) criteria, similarly to Ju *et al.* (2011). Based on these criteria, rotation corresponding to

Table 1 Limit states of piping system (Ju *et al.* 2013)

Damage State	Definition	θ_φ (radians)
Minor Damage (First Leak)	$\varphi = 2\theta$	0.0135
Moderate Damage	$\varphi = 2.5\theta$	0.0175
Severe Damage	$\varphi = 3\theta$	0.0217

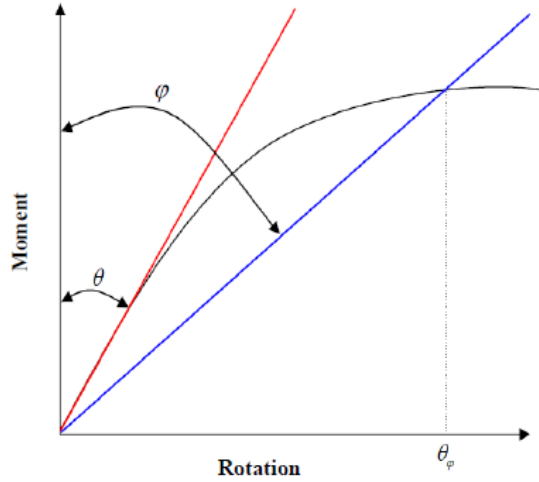


Fig. 6 Twice Elastic Slope (TES) criteria (Ju *et al.* 2011)

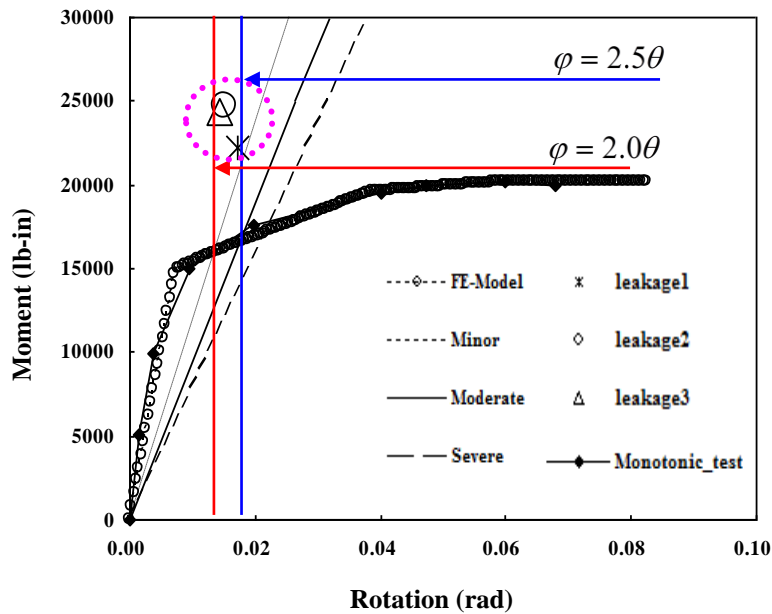


Fig. 7 Damage measure (Limit State) of 2-inch threaded T-joint System (Ju *et al.* 2011)

plastic collapse θ_ϕ can be determined by the abscissa of the point at which a line with twice the elastic slope intersects the moment-rotation curve. This condition is illustrated in Fig. 6, where $\phi = 2\theta$.

In Fig. 7, the rotations of the left spring corresponding to the “First-Leak” damage state in three cyclic tests are plotted along with the moment-rotation relationships derived from the experimentation. It is apparent that all 3 of the failure rotations lay between the lines $\phi = 2\theta$ and

$\varphi = 2.5\theta$, where θ is the elastic slope. From this result, it can be conservatively assumed that the TES ($\varphi = 2\theta$) criterion is the limit state corresponding to "First Leak". However, the same argument can be extended to define other damage states in terms of the elastic slope. Table 1 lists the various damage states considered in the structural fragility analysis of the T-joint system.

5. Analysis of piping fragility as function of interaction with building system

The seismic fragility evaluation of the piping system developed in the present study was based on multiple nonlinear time-history analyses as a function of uncertainties such as magnitude, soil type, and epicenters. The seismic fragility curves were obtained as follows. First, seismic ground

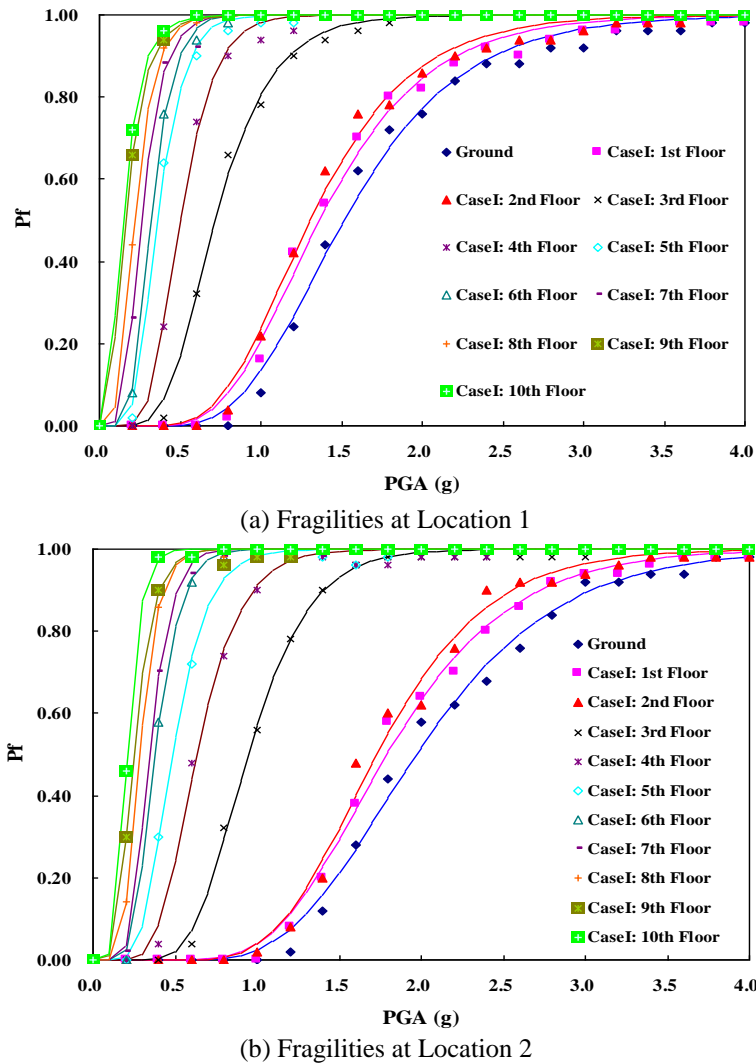
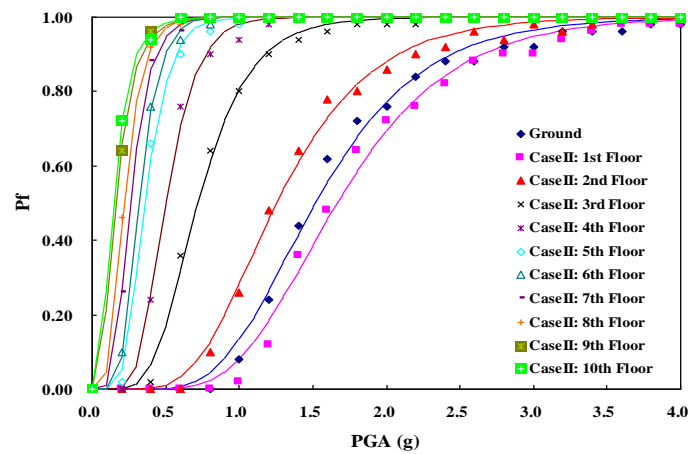


Fig. 8 Seismic fragilities of piping system installed in building without dampers

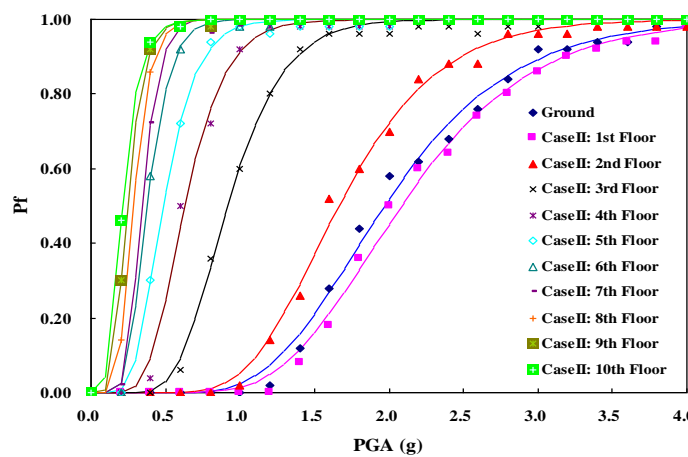
motions (50 earthquakes) were selected, and ground accelerations were obtained from the three different buildings by linear time-history analyses normalized to the same PGA levels. Second, each ground acceleration set in the 10-story building was applied to the multi-branch piping system according to the PGA level, and nonlinear time-history analyses were performed by *OpenSees* (2011), which is the Tcl/Tk-interpreter-extension-based structural analysis utility of the FE package. Third, the absolute maximum inelastic rotations were obtained, and finally, the piping fragilities in terms of the three building types were determined by Eq. (3) and the lognormal cumulative distribution function.

5.1 Piping fragility: Building without any seismic retrofit (Case I)

Fig. 8(a) plots the results of the piping system’s failure probability corresponding to the First Leak damage state at location 1 in an MDOF building without any seismic retrofit. In a similar manner, Fig. 8(b) plots the seismic fragilities determined for the second branch component of the



(a) Fragilities at Location 1



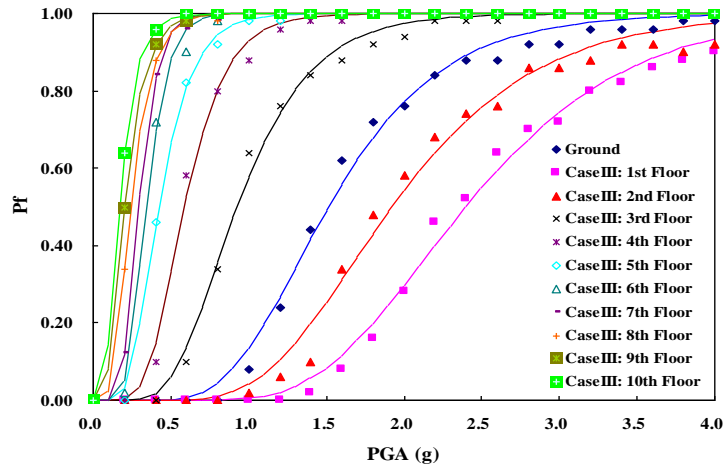
(b) Fragilities at Location 2

Fig. 9 Seismic fragilities of piping system installed in building with distributed dampers

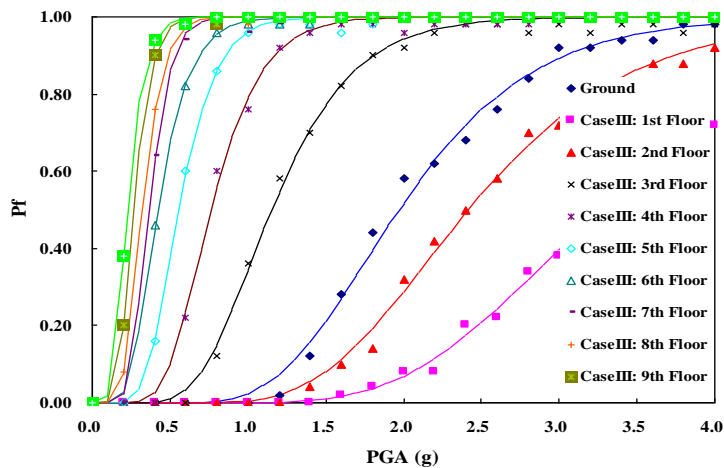
piping system. The probability of piping system failure at locations 1 and 2 of the piping system increased as the floor increased in the MDOF building, as indicated in Figs. 8(a) and 8(b). Moreover, the results showed that the fragilities at the high-level floors were significantly increased in comparison with the corresponding damage states at the low-level floors in the building system.

5.2 Piping fragility: Building with distributed dampers (Case II)

The building system subjected to seismic ground motions was retrofitted by 21 linear viscous dampers linearly distributed. Once again, the probability of piping system failure increased with increasing floor level, except for the first floor, as seen in Figs. 9(a) and 9(b). On that first floor, the seismic fragilities at locations 1 and 2 were lower than in case I; the maximum probability difference between cases I and II on the first floor was approximately 22%. As for the probabilities



(a) Fragilities at Location 1



(b) Fragilities at Location 2

Fig. 10 Seismic fragilities of piping system installed in building with optimized damper allocation

Table 2 Median peak ground acceleration (PGA) capacities

Story	Location 1 (g)			Location 2 (g)		
	Case I	Case II	Case III	Case I	Case II	Case III
1	1.37	1.67	2.40	1.80	2.10	3.28
2	1.31	1.26	1.93	1.74	1.70	2.42
3	0.72	0.72	0.93	0.96	0.92	1.16
4	0.50	0.50	0.59	0.66	0.64	0.78
5	0.36	0.36	0.43	0.50	0.50	0.56
6	0.32	0.32	0.34	0.38	0.38	0.42
7	0.26	0.26	0.30	0.36	0.36	0.38
8	0.22	0.22	0.24	0.30	0.30	0.32
9	0.16	0.16	0.20	0.26	0.26	0.28
10	0.15	0.15	0.17	0.22	0.22	0.24

of failure, they were, again excepting the first floor, very similar to the case I results. It was concluded that the distributed damper systems on the building system's first floor effected a large energy absorption.

5.3 Piping fragility: Building with optimal dampers (Case III)

Next, the optimal damper systems based on the maximum drift ratio (1.5 cm) were allocated within the building. Figs. 10(a) and 10(b) show that the probabilities of failure at locations 1 and 2 on the top floor were higher than those on the other floors, similarly to the case I- and case II-type buildings. In other words, the piping fragilities showed the same trend among the three types of building: the probability of failure increased as the floor level increased. Conversely, the piping fragilities were significantly reduced by the effect of the optimized damper allocations at the lower floor levels. For example, the fragility differences between case III and cases I and II, at both locations 1 and 2, were approximately 50% and 40%, respectively. The median PGA capacities (i.e., 50% probability of failure) for locations 1 and 2 are listed in Table 2.

6. Conclusions

This study evaluated the seismic fragility of a piping system installed in building systems subjected to 50 earthquake ground motions as a function of uncertainty. The buildings were classified into three types: 1) without any seismic retrofit; 2) with distributed linear viscous damper systems; 3) with optimized allocation of linear viscous dampers. The fragility results showed that the respective interactions between the piping and building systems corresponded to the building types. That is, the fragility results reflected the effects of the damper systems in the seismic-retrofitted buildings. The major conclusions of this paper are as follows. First, the piping fragilities at both locations 1 and 2 increased as the floor level increased. The damper control systems located at the two retrofitted buildings' lower floor levels were certainly effective; and, as expected, the piping system installed in the building without any seismic retrofit was the most

vulnerable. According to those two buildings' retrofitting, the case II piping system (distributed damper locations) was more vulnerable than the case III one (optimized damper locations). It was noted that the effects of the damper systems in both cases II and III were insignificant as the floor level increased, due to the large ground acceleration, (i.e., due to the ground-acceleration sensitivity of the piping system components). Certainly, the piping fragility analysis results presented in this paper will be used to improve the seismic performances of piping systems as retrofitted and strengthened.

Acknowledgements

This work was supported by the National Research Foundation of Korea (NRF) grant funded by the Korean government (MEST) (No. 2012-0008762).

References

- ASME (2004), Rule for Construction of Nuclear Facility Components, ASME Boiler and Pressure Vessel Code, Section III, American Society of Mechanical Engineers.
- Bachman, R., Bonowitz, D., Caldwell, P.J., Filiatrault, A., Kennedy, R.P., McGavin, G. and Miranda, E. (2004), "Engineering demand parameters for nonstructural components", *ATC-58 Project Task Report-ATC*, Redwood City, California.
- Balasubramanian, S.R., Balaji Rao, K., Meher Prasad, A., Goswami, R. and Anoop, M.B. (2014), "A methodology for development of seismic fragility curves for URBM buildings", *Earthq. Struct.*, **6**(6), 611-625.
- Dow, J. (2010), "Testing and analysis of iron and plastic T-joint in sprinkler systems", *NEESR-GC: simulation of the seismic performance of nonstructural systems*, http://nees.org/site/oldnees/filedir_2/REU2009_Dow_Paper.pdf.
- Gould, N.C. and Griffin, M.J. (2002), "The Value of Seismically Installing and Strengthening Non-Structural Equipment and Systems to Significantly Reduce Business Interruption Losses", *Proceedings of Seminar on Seismic Design, Performance, and Retrofit of Nonstructural Components in Critical Facilities*, ATC-29-2, Newport Beach, California
- Garcia, D.L. and Soong, T.T. (2002), "Efficiency of a simple approach to damper allocation in MDOF structures", *J. Struct. Control*, **9**(1), 19-30.
- Gardoni, P. and Trejo, G. (2013), "Probabilistic seismic demand models and fragility estimates for reinforced concrete bridges with base isolation", *Earthq. Struct.*, **4**(5), 525-555
- Ju, B.S., Taninada, S.T. and Gupta, A. (2011), "Fragility analysis of threaded T-Joint connections in hospital piping systems", *Proceedings of the ASME 2011 Pressure Vessel and Piping Division Conference*, Baltimore, Maryland, USA.
- Ju, B.S. and Jung, W.Y. (2013), "Seismic fragility evaluation of multi-branch piping systems installed in critical low-rise buildings", *Disaster Adv.*, **6**(4), 59-65.
- Ju, B.S., Jung, W.Y. and Ryu, Y.H. (2013), "Seismic fragility evaluation of piping system installed in critical structures", *Struct. Eng. Mech.*, **46**(3), 337-352.
- Karantoni, F., Tsionis, G., Lyrantzaki, F. and Fardis, M.N. (2014), "Seismic fragility of regular masonry buildings for in-plane and out-of-plane failure", *Earthq. Struct.*, **6**(6), 689-713.
- Kennedy, R.P., Cornell, C.A., Campbell, R.D., Kaplan, S. and Perla, H.F. (1980), "Probabilistic seismic safety study of an existing nuclear power plant", *Nuclear Eng. Des.*, **59**(2), 315-338.
- Kibboua, A., Naili, M., Benouar, D. and Kehila, F. (2011), "Analytical fragility curves for typical algerian reinforced concrete bridge piers", *Struct. Eng. Mech.*, **39**(3), 411-425.

- Kircher, C.A. (2003), "It makes dollars and sense to improve nonstructural system performance", *Proceedings of Seminar on Seismic Design, Performance, and Retrofit of Nonstructural Components in Critical Facilities*, ATC-29-2, Newport Beach, California.
- Mehani, Y., Bechtoula H., Kibboua, A. and Naili, M. (2013), "Assessment of seismic fragility curves for existing RC buildings in Algiers after the 2003 Boumerdes Earthquake", *Struct. Eng. Mech.*, **46**(6), 791-808.
- NFPA-13, Standard for the installation of Sprinkler System, National Fire Protection Association, MA, 2007 Edition.
- OpenSees (2011), Open System for Earthquake Engineering Simulation. <http://opensees.berkeley.edu/>
- Park, J. and Choi, E. (2011), "Fragility analysis of track-on steel-plate-girder railway bridge in Korea", *Eng. Struct.*, **33**(3), 696-705
- Parulekar, Y.M., Reddy, G.R., Vaze, K.K., Ghosh, A.K., Kushwaha, H.S. and Ramesh Babu, R. (2009), "Seismic response evaluation of safety related nuclear structure with yielding dampers using linearization techniques", *20th International Conference on Structural Mechanics in Reactor Technology (SMiRT-20)*.
- Perotti, F., Domaneschi, M. and De Grandis, S. (2013), "The numerical computation of seismic fragility of base-isolated nuclear power plants buildings", *Nuclear Eng. Des.*, **262**, 189-200.
- Porter, K. and Bachman, R. (2006), "Developing fragility functions for building components for ATC-58", ATC-58 Nonstructural Products Team, <http://www.sparisk.com/pubs/Porter-2006-deriving-fragility.pdf>.
- Reitherman, R. and Sabol, T.A. (1995), "Northridge earthquake of January 17, 1994: reconnaissance report-nonstructural damage", *Earthq. Spectra*, EERI, **11**, 453-514.
- SMACNA (2003), *Seismic Restraint Manual Guidelines for Mechanical Systems*, Sheet Metal and Air Conditioning Contractors' National Association, Inc.
- UBC (1997), *Uniform Building Code Vol. 2*, International Conference of Building Officials.